11th World Congress on Computational Mechanics (WCCM XI)
5th European Conference on Computational Mechanics (ECCM V)
6th European Conference on Computational Fluid Dynamics (ECFD VI)
E. Oñate, J. Oliver and A. Huerta (Eds)

MULTIPHASE FLOW MODELLING OF EXPLOSIVE VOLCANIC ERUPTIONS USING AN ADAPTIVE UNSTRUCTURED MESH-BASED APPROACH

Christian T. Jacobs[1,*], Gareth S. Collins[1], Matthew D. Piggott[1] and Stephan C. Kramer[1]

[1] Department of Earth Science and Engineering
Imperial College London
London, SW7 2AZ, United Kingdom
e-mail: c.jacobs10@imperial.ac.uk, web page: http://amcg.ese.ic.ac.uk/

Key words: Multiphase Flow, Mesh Adaptivity, Volcanic Eruptions

Abstract. Explosive volcanic eruption events, in which large quantities of hot gas and ash are expelled high into the atmosphere, are one of the most powerful natural hazards. In order to gain a full understanding of the dangers these eruptions pose, their complex multiscale and multiphase nature must be captured to a high degree of accuracy. The application of numerical multiphase flow models often represents the only tenable way of achieving this, and permits the investigation of ash cloud evolution in domains many times larger than the laboratory-scale. However, even the most advanced models of eruption dynamics are restricted by the fixed mesh-based approaches that they generally employ. The research presented herein introduces a compressible multiphase flow model recently implemented within Fluidity, a combined finite element / control volume CFD code, for the study of explosive volcanic eruptions. Fluidity adopts an adaptive unstructured mesh-based approach to discretise the domain and focus numerical resolution only in areas important to the dynamics, while decreasing resolution where it is not needed as a simulation progresses. This allows the accurate but economical representation of the flow dynamics throughout time. The application of the model considers a 7 km $\times$ 7 km domain in which the violent eruption of hot gas and volcanic ash high into the atmosphere is simulated. It is shown by a convergence analysis that Fluidity offers the same solution accuracy for reduced computational cost using an adaptive unstructured mesh, compared to the same simulation performed with a fixed uniform mesh.

1 INTRODUCTION

The study of multiphase flow is an exciting yet challenging area of fluid mechanics. Concerned with how two or more states of matter mix and interact when subjected to

various forces, it provides much-needed insight into the behaviour of natural phenomena. One prominent geophysical example is an explosive volcanic eruption of searing hot gas and solid ash particles being ejected high into the atmosphere. The resulting particle-laden cloud is known as a volcanic plume [1], which can later collapse to form ground-hugging density currents capable of tremendous speed. Such events are often widely publicised because of their hazardous, destructive and unpredictable nature, causing high death tolls and massive damage to the surrounding area. In order to make well-founded predictions about the hazards volcanoes pose and to aid the interpretation of the ash fallout, a good understanding of the whole physical system is required.

The development and application of numerical multiphase flow models has significantly advanced the understanding of eruption events because of their potential to resolve the multiple scales present in nature, extend the results of experiments and field studies to larger domains, and incorporate a vast amount of complexity (see e.g. [2, 3, 4]). One crucial aspect of any numerical model is the discretisation of the domain into a finite number of cells, forming a mesh, where the properties of the flow such as velocity are approximated upon the solution nodes. This is directly related to both accuracy and computational footprint; more cells (or nodes) give better accuracy but at the cost of increased simulation runtime. As a result of this correlation, some of even the most advanced multiphase flow models are restricted to relatively small, simple and often two-dimensional domains focussed around the vent of the volcano [5].

Most existing approaches for volcanic eruption modelling consider either a fixed structured mesh or a fixed unstructured mesh. Structured meshes are characterised by a rigid checkerboard-like layout of solution nodes, with each node being connected to its nearest neighbours using a simple formula. Since the numerical resolution is inherently uniform in all or part of the domain, a large number of superfluous nodes can exist. In contrast, unstructured meshes have the advantage that nodes can be arbitrarily connected to one another, thus providing the freedom for the resolution to increase or decrease only where desired [6] and allowing the construction of meshes that conform well to the topography [7]. For example, early on in a volcanic eruption simulation, high accuracy may only be desired near the vent of the volcano; what happens 20 kilometres away is not yet likely to be of interest so resolution can be decreased in that region. However, a fixed unstructured mesh which concentrates resolution in a region of interest in the flow, such as around a growing volcanic plume, will no longer be optimal when this plume changes its position or size and moves out of the region of high resolution. The reduced accuracy resulting from this can dramatically affect the numerical solution. To overcome this issue, high resolution would need to be placed in areas where it is not always needed, in order to pre-empt the position of the plume or other dynamics throughout time. Just like fixed structured meshes, this would yield a large number of superfluous nodes that severely restrict the efficiency of the model, particularly when the positions of the important flow structures are not known *a priori*. Improved numerical approaches must be therefore be devised if the full system is to be modelled in detail with available computational resources.

In contrast to the fixed mesh approaches adopted by most existing models of volcanic eruptions, the work presented in this paper describes a compressible multiphase flow model recently implemented within Fluidity, an open-source, combined finite element / control volume CFD code, which features an *adaptive* (unstructured) mesh-based approach [8]. Such an approach has the potential to supply finer numerical resolution only in areas important to the dynamics being studied and coarser resolution in those areas that are not, thereby minimising the number of superfluous solution nodes. As the flow progresses the mesh is periodically optimised through a series of local topological operations (such as node addition and edge flipping) to accurately, but efficiently, represent the flow domain throughout time [9]. This approach has already brought significant benefits to numerical models; for example, it has been shown that an adaptive unstructured mesh can yield results equally accurate as those produced with a fixed mesh, with more than an order of magnitude fewer nodes [10, 11]. This in turn has brought similar benefits including faster runtimes and reduced computational costs over simulations performed with a uniformly fine mesh [9, 11]. Clearly the use of an adaptive unstructured mesh-based approach is potentially very fruitful for modelling multiphase geophysical flows occurring on a wide range of scales in complex domains.

The structure of the paper is as follows. Section 2 details the model equations describing the laws of conservation of mass, momentum and energy, and briefly states the discretisation methods employed. The interested reader is referred to the thesis by Jacobs [12], from which most of the content in this paper is based, for further details about the discretisation, verification and validation of the model. Section 3 presents the model's application which involves 2D simulations of a volcanic eruption of hot gas and ash being ejected high into the atmosphere in a kilometre-scale domain. The efficacy of the adaptive unstructured mesh approach is illustrated with a convergence analysis of the volcanic fountain height. The paper then closes with some concluding remarks in Section 4.

2 MODEL EQUATIONS

The work presented in this paper focusses on multiphase flows that comprise a single continuous phase (a connected liquid or gas substance) in which one or more dispersed phases (comprising a finite number of solid particles, liquid droplets and/or gas bubbles) are immersed [13]. The applications of the multiphase flow model are such that the continuous phase will always be a compressible gas, and the dispersed phase comprising solid ash particles will be treated as incompressible.

2.1 Momentum equation

The equation describing the law of conservation of momentum for phase $i = 1, 2, \ldots, N$ (where N is the total number of phases) is given in non-conservative form by [13]

$$\alpha_i \rho_i \frac{\partial \mathbf{u}_i}{\partial t} + \alpha_i \rho_i \mathbf{u}_i \cdot \nabla \mathbf{u}_i = -\alpha_i \nabla p + \alpha_i \rho_i \mathbf{g} + \nabla \cdot (\alpha_i \tau_i) + \mathbf{f}_i. \tag{1}$$

The terms α_i, ρ_i, and $\mathbf{u_i}$ are the volume fraction, density and velocity of phase i, respectively. The terms p and τ_i represent the (shared) pressure and viscous stress acting on phase i, and $\mathbf{g}$ is the gravitational vector. The inter-phase momentum exchange term $\mathbf{f}_i$ models only the fluid-particle drag force (using the drag correlation by Wen & Yu [14] throughout) because of the relatively dilute nature of the flow (α_d is of $O(10^{-3})$).

2.2 Continuity equation

By assuming that all phases share a common pressure field, only one 'bulk' continuity equation is required to describe the law of conservation of mass. This is derived by adding together the continuity equation of each of the N phases, such that

$$\alpha_1 \frac{\partial \rho_1}{\partial t} + \rho_1 \left(\sum_{i=2}^{N} \nabla \cdot (\alpha_i \mathbf{u}_i) \right) + \nabla \cdot (\alpha_1 \rho_1 \mathbf{u}_1) = 0. \tag{2}$$

Note that the continuous phase is identified by the index $i = 1$ here.

2.3 Internal energy equation

The third governing equation describes the conservation of energy law. For convenience, this work considers the specific internal energy of a system e_i (in other words, the internal energy per unit mass), and the energy equation for phase i used in the work presented here is given by

$$\alpha_i \rho_i \frac{\partial e_i}{\partial t} + \alpha_i \rho_i \mathbf{u}_i \cdot \nabla e_i = -\nabla \cdot (\alpha_i \mathbf{q}_i) + Q_i, \tag{3}$$

where Q_i represents the heat transfer to phase i from the other $N - 1$ phases, and $\mathbf{q}_i$ is the heat flux of phase i [13, 15]. The heat transfer correlation by Gunn [16] is used in this work to parameterise the inter-phase energy exchange term Q_i.

2.4 Equation of state

This work uses the ideal gas equation of state to determine the pressure field from other flow variables [17]:

$$p = (\gamma_c - 1) e_c \rho_c, \tag{4}$$

where the subscript c denotes properties of the continuous phase, and γ_c is the ratio of specific heats.

2.5 Discretisation and solution method

The continuity, momentum and energy equations are discretised in Fluidity using the Galerkin finite element method (for the spatial discretisation) and the implicit backward Euler method (for the temporal discretisation). Throughout this paper, the velocity field is represented by piecewise linear basis functions, while the pressure, density and internal energy fields are represented by piecewise constant basis functions. This choice forms the

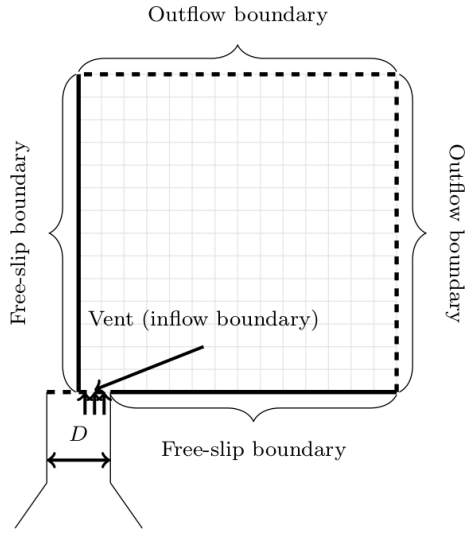

Figure 1: Illustration of the 7 km × 7 km domain used in the volcanic eruption simulations. The volcano's vent has diameter D. Only half of the vent is considered in the model, such that the inflow boundary condition has length $D/2$.

so-called P1-P0 velocity-pressure element pair. The advection equation used to advect the volume fraction fields is discretised using a control volume method, in conjunction with a first-order upwinding technique used to evaluate the advection term at the boundaries of each control volume [18, 8]. The discretisation process, the explicit solution method, the non-linear Picard iteration scheme used, and the verification and validation of the model are described in detail by Jacobs [12].

3 APPLICATION TO VOLCANIC ERUPTIONS

The application of the compressible multiphase flow model concerns the two-dimensional simulation of explosive volcanic eruptions and the dynamics of the resulting ash plumes. The setup and results are discussed herein.

3.1 Simulation set-up

The two-dimensional domain was a 7 km × 7 km square (a vertical slice in the x-z plane), illustrated in Figure 1. It was assumed that the volcano and the erupting plume were axisymmetric about the midpoint of the vent (with diameter $D = 400$ m), such that only half of the vent of the volcano was considered. Simulations were run using both fixed and adaptive meshes.

Four fixed structured meshes and four fixed unstructured meshes were created using Gmsh [19] with characteristic element lengths of 200 m, 100 m, 50 m, and 25 m. The elements of each mesh were triangular. The time-steps were respectively set to 0.04 s, 0.02 s, 0.01 s, and 0.005 s to maintain a near-constant upper bound on the Courant number of approximately 0.1. For the adaptive unstructured mesh case, the maximum

and minimum element length constraints were set to 7 km and 5 m, respectively (i.e. well above/below the resolution of the fixed meshes). Although these bounds were never reached, the adaptive mesh simulations were allowed to use element lengths much smaller than those in the fixed mesh simulations which potentially permitted greater accuracy, whilst at the same time using much larger element lengths in places where resolution could be reduced to potentially reduce computational costs. The mesh was adapted every 10 time-steps and used interpolation error bounds to control the amount of refinement [10, 11]: the error bound for the volume fraction field α_d was varied between 0.005 and 0.16 in order to capture the ash plume, and the error bound for the air density ρ_c was varied between 0.4 and 12.8 kgm^{-3} to capture the initial blast wave from the eruption. Consistent interpolation was used as a quick and bounded technique to copy across the solution from the pre-adapt to the post-adapt mesh [20]. The time-step was fixed at 0.005 s which maintained an upper bound on the Courant number of about 0.3.

All simulations were performed until $t = 120$ s which was adequate time to show all the main flow characteristics. The non-linear Picard iteration loop terminated once $\max(||\mathbf{u}_c^k - \mathbf{u}_c^{k-1}||_2) \leq 10^{-4}$, $\max(||\mathbf{u}_d^k - \mathbf{u}_d^{k-1}||_2) \leq 10^{-4}$, and $\max(|p^k - p^{k-1}|) \leq 10^{-4}$, for some non-linear iteration k, was reached. This number k was typically between 4 and 15.

The physical parameters were as follows: ratio of specific heats $\gamma_c = 1.4$, air viscosity $\mu_c = 1.85 \times 10^{-5}$ Pas, solids viscosity $\mu_d = 0.5$ Pas, specific heat of air $C_{v,c} = 718$ Jkg^{-1}K^{-1}, specific heat of ash particles $C_{v,d} = 954$ Jkg^{-1}K^{-1}, thermal conductivity of air $k_c = 0.05$ Wm^{-1}K^{-1}, thermal conductivity of ash particles $k_d = 2.2$ Wm^{-1}K^{-1}, ash density $\rho_d = 2{,}400$ kgm^{-3}, and particle diameter $d_d = 2 \times 10^{-4}$ m. These values were within the range of those used by Valentine & Wohletz [21], Neri *et al.* [2] and Pelanti [22]. In reality, many of the physical parameters are functions of temperature, namely viscosity and specific heat. However, in this work, they were all assumed to be constant. For simplicity, water vapour content was also neglected such that the erupting gas was composed solely of dry air, and only one particle size was considered.

3.2 Initial and boundary conditions

The initial temperature of both phases was set to 288.15 K. A zero initial velocity field was set for both phases; no wind effects were modelled in the gas phase. The initial pressure profile followed an exponential decrease with height y, such that

$$p = p_0 \exp\left(\frac{-|\mathbf{g}|y}{(\gamma_c - 1)\, e_c}\right), \tag{5}$$

where $p_0 = 101{,}325$ Pa.

The Dirichlet boundary conditions employed closely matched those used in [21]. The continuous and dispersed phase were assumed to be in both kinetic and thermal equilibrium; a constant temperature $T_{\text{vent}} = T_c = T_d$ of 1,200 K was assumed at the vent which corresponded to internal energies of $e_c = 206,891.7$ Jkg^{-1} and $e_d = 274,895.1$ Jkg^{-1}. A constant vertical velocity $\mathbf{u}_{\text{vent}} = \mathbf{u}_c = \mathbf{u}_d$ of 80 ms^{-1} was imposed at the vent along with

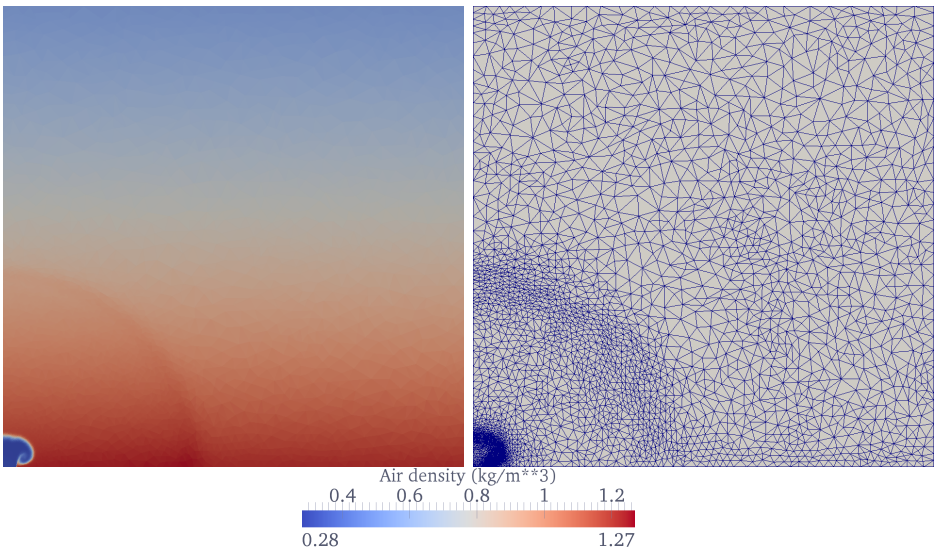

Figure 2: Density of air ρ_c at $t = 10$ s in the highest-resolution adaptive mesh simulation. Hot low density air entered the domain at 80 ms^{-1}, and the blast wave generated from the explosive eruption travelled towards the top and right-hand side boundaries at approximately 300 ms^{-1}. The mesh adapts to the shock front as well as the growing plume. The image shows the whole 7 km $\times$ 7 km domain.

a volume fraction α_d of 10^{-3} for the dispersed phase, which was within the range of values considered in the parameter study by Valentine & Wohletz [21].

A free-slip boundary condition for both phases preserved the symmetry of the problem along the y-axis, and another free-slip boundary condition along the ground was also employed. No conditions were imposed on the velocity of either phase along the outflow. Instead, a pressure boundary condition that agreed with the hydrostatic pressure profile was enforced there. At the vent, a pressure boundary condition of $p = 101,325$ Pa was imposed.

3.3 Results

The qualitative results from Fluidity compare well with the flow features and behaviour observed in numerical simulations of explosive volcanic eruptions presented in the literature [2, 3, 4, 21, 22]. As the volcano erupted, ash particles and hot air entered the domain at 80 ms^{-1}. The abrupt high inlet velocity caused a (sub-sonic) hemispherical shock wave to be generated that propagated outwards from the vent with an approximate speed of 300 ms^{-1}, as shown in Figure 2. As the plume of hot gas and ash grew and travelled vertically upwards, fluid-particle drag effects caused the head of the plume to become bulbous-shaped and an overhanging vortex began to noticeably form.

The eruption column continued to rise until a height of approximately 700 m above ground level, after which it began to collapse as its bulk density became greater than that of the ambient atmospheric air and the up-thrust from the vent could not longer sustain its growth. The erupting column of volcaniclastic material became somewhat like

a fountain. The falling ash particles first hit the ground at $t \approx 45$ s. The majority of the settling particles created a dense, ground-hugging current that travelled radially outwards at high-speed, known as a pyroclastic flow, while some became entrained and recycled in the eruption column along with the surrounding ambient air as shown in Figure 3. This entrainment process formed the recirculating region. Furthermore, despite the majority of the column collapsing, a thin dilute region of hot particles and low density air along the top of the column continued to rise upwards to form a second smaller plume above the fountain, referred to as the convective region. As a result of the height and the dilute nature of the region, the bulk density was less than that of the ambient atmosphere which allowed buoyancy effects to dominate the dynamics. It is worth noting that, in comparison with the structured fixed mesh simulations, the use of an unstructured mesh appeared to stunt the growth of this convective region. These effects were caused by the unstructured nature of the mesh itself which introduced uneven perturbations in the flow through numerical diffusion.

All pyroclastic flows eventually lose enough momentum and begin to deposit material. While a dense layer of particles forms at the base, convective instabilities can occur in the dilute region along the top of the flow as the bulk density of the hot gas-particle mixture becomes less than the ambient density there. The loss of momentum allows buoyancy effects to dominate, which in turn allows small particle plumes to grow along the upper layer of the pyroclastic flow [4]. These can later merge and ascend as larger dilute clouds, and are referred to as coignimbrite or phoenix plumes. The fact that these coignimbrite plumes did not form in the numerical presentations may have been due to the simple topography of the domain which did not cause enough momentum loss to allow buoyancy effects to dominate. At the end of the simulation the pyroclastic flow was still moving at considerable speed, thus potentially hindering the formation of coignimbrite plumes. Despite this, all other key structures found in a typical explosive volcanic eruption were present and adequately represented which provides at least some confidence in the plausibility of the numerical results.

To test the efficacy of the adaptive unstructured mesh approach, and to ensure that the dynamics were not brought about by numerical artefacts and were in fact representative of the physics, a convergence analysis was performed. Fixed structured and unstructured meshes, and adaptive unstructured meshes (using the element lengths and error bounds specified earlier) were all considered. It was found *a posteriori* that the height of the growing volcanic plume provided a good measure of convergence. However, this was only valid up until $t = 10$ s, after which the dynamics became too non-linear and turbulent as the plume collapsed and a recirculation region formed near the vent. In order to compare the different mesh types, the error in the height of the fountain after $t = 10$ s was plotted against the characteristic element length (for the fixed meshes only) in Figure 4a, and also against the maximum number of solution nodes used (during the first 10 s of simulation time) in the mesh in Figure 4b. The error was relative to the fountain height found in the simulation using the finest mesh of the same mesh type. For example, the error from

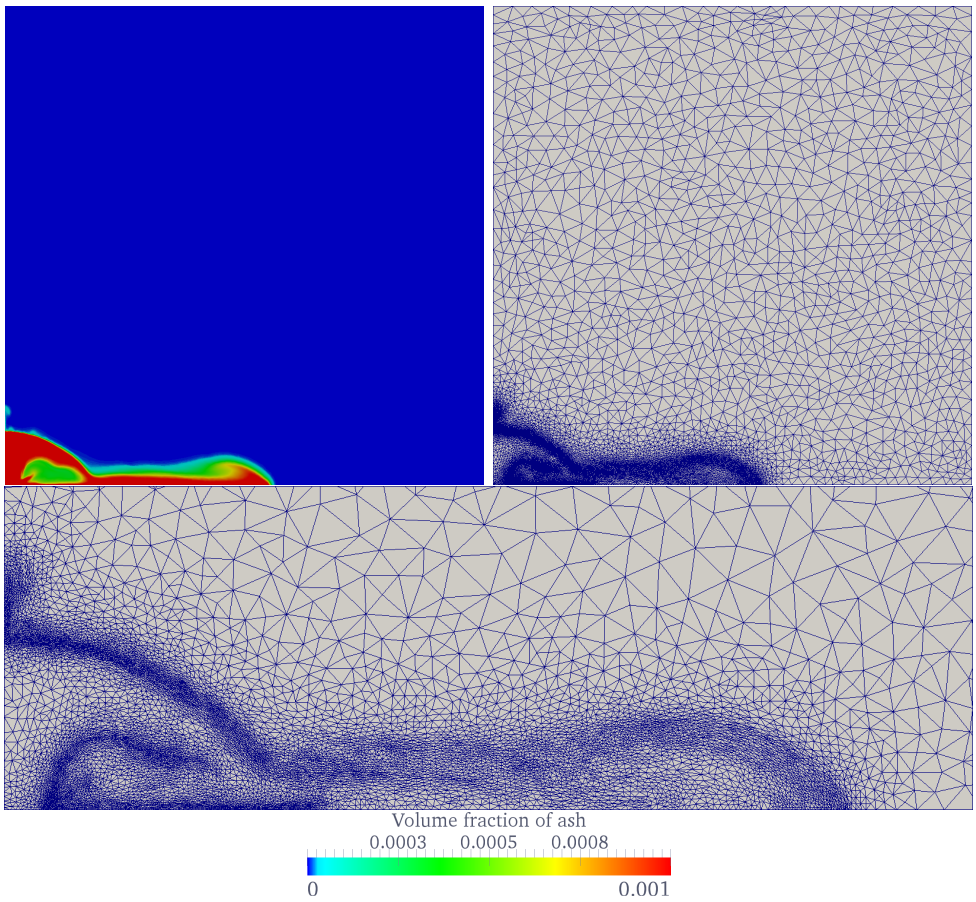

Figure 3: Volume fraction of ash particles α_d at $t = 80$ s in the highest-resolution adaptive mesh simulation. The bottom image shows the mesh in a 4.5×1.5 km section around the vent. This illustrates the refinement around the important flow structures, and also shows the growth of a small buoyant cloud of particles which formed the convective region above the main fountain of hot gas and ash.

the 200 m fixed structured mesh simulation was compared with the error from the 25 m fixed structured mesh simulation. The height of the fountain was defined as the highest point where the bulk density of the gas-particle mixture became equal to the ambient atmospheric density. All simulations were run in parallel over two dual-core Intel Xeon E5430 processors with at least 8 GB of free RAM shared between them.

The suite of Fluidity simulations converged to a steady-state fountain height of approximately 500 m. A convergence rate between first-order and second-order was obtained, with more than an order of magnitude fewer nodes being needed in the adaptive unstructured mesh case to represent the solution to the same degree of accuracy. In terms of run-time, the fixed mesh simulations that used a 50 m resolution took approximately 93 hours and 80.5 hours (for the unstructured and structured versions, respectively), while the adaptive unstructured mesh simulation of comparable accuracy took just 18 hours to run to completion. This is clearly a significant saving, and helps to illustrate the benefits

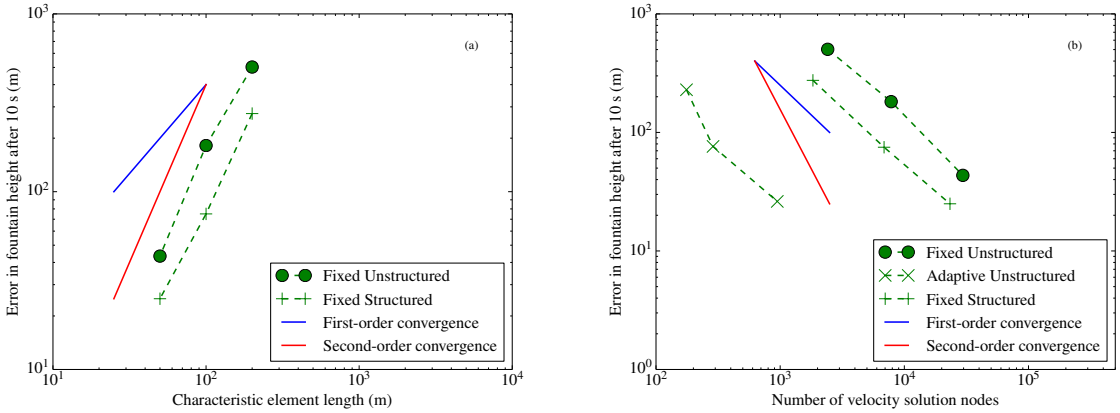

Figure 4: Error in the fountain height at $t = 10$ s, relative to the simulation using the finest resolution, against (a) the characteristic element length (for fixed meshes only) and (b) the number of solution nodes in the fixed and adaptive meshes. Note that in the case of the adaptive unstructured mesh simulations, the maximum number of nodes used during the time period [0, 10] s is plotted.

of adopting an adaptive unstructured mesh approach. As the complexity is increased and simulations become more demanding, it can become infeasible for traditional fixed mesh approaches to tackle such multi-scale problems. The effectiveness of an adaptive unstructured mesh approach therefore becomes even more pronounced when moving from a simple 2D square domain to a full 3D domain with realistic topography in the vicinity of the volcano, and when additional realism such as multiple dispersed phases, multiphase turbulence parameterisation, and atmospheric forcing is included. However, factors such as the additional numerical diffusion introduced by the post-adapt solution interpolation routine, and the extra costs associated with a more complicated implementation, must also be taken into account when deciding to use such an approach.

4 CONCLUSIONS

- A compressible multiphase flow model, implemented in the Fluidity CFD code, was presented. The model was applied to simulate an explosive volcanic eruption (an example of a scenario that is more suitable for an adaptive unstructured mesh since the dynamics are complex and multi-scale, but often only require fine resolution to be placed in a relatively small portion of the domain, especially at early times).

- Key components of a typical eruption event (the initial shock wave, ash fountain, recirculating and convective regions, and pyroclastic flow) were all successfully captured and their dynamics were qualitatively similar to that observed in nature.

- For a quantitatively similar degree of accuracy based on a convergence analysis of the volcanic fountain height, the simulations that used an adaptive unstructured mesh required an order of magnitude fewer nodes and were faster relative to the

same simulation run using a fixed-mesh based approach.

- Numerical multiphase flow models such as the one presented in this paper continue to pave the way forward with regards to understanding more about the dynamics of volcanic ash transport and other complex natural phenomena. The benefits that an adaptive unstructured mesh-based approach can bring to such models, demonstrated here, will hopefully encourage further advances in numerical modelling techniques.

5 ACKNOWLEDGEMENTS

CTJ and SCK were funded by the Institute of Shock Physics at Imperial College London and the Atomic Weapons Establishment; GSC was funded by the Natural Environment Research Council, Fellowship Grant NE/E013589/1. Support from the Imperial College High Performance Computing Service was also gratefully received.

REFERENCES

[1] R. S. J. Sparks. The dimensions and dynamics of volcanic eruption columns. *Bulletin of Volcanology*, 48(1):3–15, 1986.

[2] A. Neri, T. Esposti Ongaro, G. Macedonio, and D. Gidaspow. Multiparticle simulation of collapsing volcanic columns and pyroclastic flow. *Journal of Geophysical Research*, 108(B4), 2003.

[3] F. Dobran, A. Neri, and G. Macedonio. Numerical Simulation of Collapsing Volcanic Columns. *Journal of Geophysical Research*, 98(B3):4231–4259, 1993.

[4] A. Neri and G. Macedonio. Numerical simulation of collapsing volcanic columns with particles of two sizes. *Journal of Geophysical Research*, 101(B4):8153–8174, 1996.

[5] C. Textor, Hans-F. Graf, A. Longo, A. Neri, T. Esposti Ongaro, P. Papale, C. Timmreck, and G.G.J. Ernst. Numerical simulation of explosive volcanic eruptions from the conduit flow to global atmospheric scales. *Annals of Geophysics*, 48(4-5):817–842, 2005.

[6] M. D. Piggott, C. C. Pain, G. J. Gorman, P. W. Power, and A. J. H. Goddard. *h*, *r*, and *hr* adaptivity with applications in numerical ocean modelling. *Ocean Modelling*, 10(1-2):95–113, 2006.

[7] G. J. Gorman, M. D. Piggott, C. C. Pain, C. R. E. de Oliveira, A. P. Umpleby, and A. J. H. Goddard. Optimisation based bathymetry approximation through constrained unstructured mesh adaptivity. *Ocean Modelling*, 12(3-4):436–452, 2006.

[8] Imperial College London. *Fluidity 4.1 Manual*, 2011. URL `http://amcg.ese.ic.ac.uk/Fluidity`.

[9] M. D. Piggott, P. E. Farrell, C. R. Wilson, G. J. Gorman, and C. C. Pain. Anisotropic mesh adaptivity for multi-scale ocean modelling. *Philosophical Transactions of the Royal Society A*, 367(1907):4591–4611, 2009.

[10] H. R. Hiester, M. D. Piggott, and P. A. Allison. The impact of mesh adaptivity on the gravity current front speed in a two-dimensional lock-exchange. *Ocean Modelling*, 38(1-2):1–21, 2011.

[11] C. T. Jacobs, G. S. Collins, M. D. Piggott, S. C. Kramer, and C. R. G. Wilson. Multiphase flow modelling of volcanic ash particle settling in water using adaptive unstructured meshes. *Geophysical Journal International*, 192(2):647–665, 2013.

[12] C. T. Jacobs. *Modelling of Multiphase Flows on Adaptive Unstructured Meshes with Applications to the Dynamics of Volcanic Ash Plumes*. PhD thesis, Imperial College London, 2013.

[13] C. T. Crowe, M. Sommerfeld, and Y. Tsuji. *Multiphase Flows with Droplets and Particles*. CRC Press, 1998.

[14] C. Y. Wen and Y. H. Yu. Mechanics of Fluidization. *Chemical Engineering Progress Symposium Series*, 62:100–111, 1966.

[15] M. Ishii. *Thermo-Fluid Dynamic Theory of Two-Phase Flow*. Eyrolles, 1975.

[16] D. J. Gunn. Transfer of heat or mass to particles in fixed and fluidised beds. *International Journal of Heat and Mass Transfer*, 21(4):467–476, 1978.

[17] R. Saurel and R. Abgrall. A Simple Method for Compressible Multifluid Flows. *SIAM Journal on Scientific Computing*, 21(3):1115–1145, 1999.

[18] C. Wilson. *Modelling Multiple-Material Flows on Adaptive Unstructured Meshes*. PhD thesis, Imperial College London, 2009.

[19] C. Geuzaine and J.-F. Remacle. Gmsh: A 3-D finite element mesh generator with built-in pre- and post-processing facilities. *International Journal for Numerical Methods in Engineering*, 79(11):1309–1331, 2009.

[20] P. E. Farrell. *Galerkin projection of discrete fields via supermesh construction*. PhD thesis, Imperial College London, 2009.

[21] G. A. Valentine and K. H. Wohletz. Numerical Models of Plinian Eruption Columns and Pyroclastic Flows. *Journal of Geophysical Research*, 94(B4):1867–1887, 1989.

[22] M. Pelanti. *Wave Propagation Algorithms for Multicomponent Compressible Flows with Applications to Volcanic Jets*. PhD thesis, University of Washington, 2005.